Neurobiology of Aging 79 (2019) 22–29

Contents lists available at ScienceDirect

Neurobiology of Aging

journal homepage: www.elsevier.com/locate/neuaging

Evolution of brain atrophy subtypes during aging predicts long-term cognitive decline and future Alzheimer's clinical syndrome

Vincent Planche [a,b,*], Pierrick Coupé [c], Catherine Helmer [d], Mélanie Le Goff [d], Helene Amieva [d], François Tison [a,b], Jean-François Dartigues [b,d], Gwénaëlle Catheline [e,f]

[a] Univ. Bordeaux, CNRS, UMR 5293, Institut des Maladies Neurodégénératives, Bordeaux, France
[b] Centre Mémoire de Ressources et de Recherches, Pôle de Neurosciences Cliniques, CHU de Bordeaux, Bordeaux, France
[c] Univ. Bordeaux, CNRS, UMR 5800, Laboratoire Bordelais de Recherche en Informatique, Talence, France
[d] Univ. Bordeaux, Inserm, UMR 1219, Bordeaux Population Health Research Center, Bordeaux, France
[e] EPHE, PSL, Bordeaux, France
[f] Univ. Bordeaux, CNRS, UMR 5287, Institut de Neurosciences cognitives et intégratives d'Aquitaine, Bordeaux, France

ARTICLE INFO

Article history:
Received 6 December 2018
Received in revised form 14 February 2019
Accepted 13 March 2019
Available online 22 March 2019

Keywords:
Hippocampus
Cortex
Imaging
Alzheimer
Aging
Cohort study

ABSTRACT

It is currently unknown whether brain atrophy subtypes defined in Alzheimer's disease are clinically relevant during aging. We investigated participants (n = 368) from a population-based cohort of non-demented older adults who received longitudinal neuropsychological assessments during 12 years. Magnetic resonance imaging scans at baseline and 4 years later were used to define participants with "hippocampal predominant atrophy," "cortical predominant atrophy," "homogenous atrophy," and "no evidence of brain subtype atrophy" based on the dynamics of hippocampal-to-cortical volume ratio evolution. After adjustment on age, gender, educational level, and ApoE4 genotype, participants with "hippocampal predominant atrophy" declined faster regarding global cognition, verbal fluency, and verbal episodic memory. In Cox proportional-hazards models, "hippocampal predominant atrophy" was associated with an increased risk of developing Alzheimer's clinical syndrome over time (hazard ratio = 5.73; 95% CI 2.71–12.15), independently of age and ApoE4 genotype, the 2 other significant predictive factors. As a possible surrogate of confined tauopathy and early Alzheimer's disease pathology, future studies should consider the definition of "hippocampal predominant atrophy" based on hippocampal-to-cortical volume ratio evolution rather than hippocampal volume alone.

1. Introduction

The neurodegenerative process causing brain atrophy and cognitive impairment in Alzheimer's disease involves both the limbic system and neocortical areas. Hence, magnetic resonance imaging (MRI) plays a key role in the clinical assessment of patients with suspected Alzheimer's disease because regional atrophy can provide positive diagnostic information (Scheltens et al., 2016). However, the pattern and dynamics of brain atrophy in Alzheimer's disease are somewhat different according age at onset, clinical presentation, neuropsychiatric comorbidities, vascular risk factors, and rate of decline (Dickerson et al., 2009, 2017).

Studies combining premortem neuroimaging and postmortem neuropathology have suggested that patterns of gray matter atrophy can be related to the topographic distribution and progression of tau neurofibrillary tangles (Gosche et al., 2002; Jack et al., 2002). Interestingly, recent cross-sectional MRI studies have been able to capture distinct neuropathologically defined subtypes of Alzheimer's disease according to the Murray-Dickson definition (Byun et al., 2015; Risacher et al., 2017; Whitwell et al., 2012). This categorization of Alzheimer's disease is based on an algorithm which classifies Alzheimer's disease cases into "typical," "hippocampal sparing," and "limbic predominant" patterns of neurofibrillary tangles distribution, using the ratio of hippocampal-to-cortical neurofibrillary tangles density (Murray et al., 2011). In these studies, a hippocampal sparing pattern of atrophy on MRI (correlating to an hippocampal sparing distribution of neurofibrillary tangles) was associated with a faster cognitive and functional decline (Murray et al., 2011; Risacher et al., 2017; Whitwell et al., 2012). However, it is currently unknown whether this rather simple categorization of brain atrophy subtypes is also clinically relevant in asymptomatic preclinical Alzheimer's disease (Dubois et al.,

* Corresponding author at: Institut des Maladies Neurodégénératives, Centre Broca Nouvelle-Aquitaine, UMR CNRS 5293, 146 rue Léo Saignat, 33076 Bordeaux, cedex, France. Tel.: +33 533 51 47 19.
E-mail address: vincent.planche@u-bordeaux.fr (V. Planche).

0197-4580/$ – see front matter © 2019 Elsevier Inc. All rights reserved.
https://doi.org/10.1016/j.neurobiolaging.2019.03.006

2014). Furthermore, none of these previous studies have really captured the dynamics of brain atrophy subtypes because they relied on cross-sectional analyses.

Although the precise timing remains elusive, due to the lack of longitudinal studies long enough at the presymptomatic stage of the disease, the current models of Alzheimer's disease pathophysiology postulate that neurofibrillary tangles appear years before the symptomatic phase of the disease (Braak and Braak, 1991; Jack et al., 2010; Sperling et al., 2011). Thus, based on the dynamics of hippocampal-to-cortical volume ratio (HV/CTV ratio) evolution, this study aims at determining whether different subtypes of brain atrophy in older adults could predict differential cognitive decline and an increased risk of Alzheimer's clinical syndrome over time. For that purpose, we studied a well-defined population-based cohort of older adults who underwent 2 MRI examinations at 4-year intervals and a neuropsychological and clinical follow-up during 12 years.

2. Methods

2.1. Study sample

The data used in the following analyses were obtained from a subset of the Bordeaux sample of the 3-city study, a longitudinal population-based cohort designed to evaluate risk factors of dementia (3C Study Group, 2003). During the 1999-2000 inclusion period, noninstitutionalized individuals aged 65 years and older were randomly recruited from electoral lists and followed prospectively for up to 12 years. From the initial cohort of participants with baseline MRI (n = 663), only nondemented participants who agreed to have a second MRI 4 years later were included in the present analyses (n = 368). Information regarding demographical characteristics and ApoE4 genotype (carriers/non carrier: at least one allele) was also collected at baseline. All participants gave written informed consent to participate and the study protocol was approved by the ethics committee of Kremlin-Bicêtre University Hospital (Paris, France).

2.2. Neuropsychological assessment and diagnosis of incident Alzheimer's clinical syndrome

During the 12-year follow-up period, neuropsychological assessments were administered by trained psychologists at baseline and after 2, 4, 8, 10, and 12 years. The battery consisted of the Mini-Mental State Evaluation (global cognitive functions), the Free and Cued Selective Reminding Test (FCSRT: verbal episodic memory [sum of the number of words retrieved at the 3 free or cued trials]), the Benton Visual Retention Test (visuospatial working memory), the Isaacs Set Test (IST: semantic fluency), and the Trail-Making Test part A and B (TMT-A and TMT-B: attention, information processing speed, and executive functions [{number of correct moves/total time}×10]).

The diagnosis of dementia was prespecified at home by a neuropsychologist, at each visit (2, 4, 8, 10, and 12 years). After this first assessment, a definitive diagnosis of dementia and of possible or probable Alzheimer's disease was made by a panel of independent neurologists according to the Diagnostic and Statistical Manual of Mental Disorders criteria and the National Institute of Neurological and Communicative Diseases and Stroke/Alzheimer's Disease and Related Disorders Association criteria (McKhann et al., 1984). They were finally labeled "Alzheimer's clinical syndrome" according to the recent National Institute on Aging and Alzheimer's Association research framework recommendations (Jack et al., 2018a).

2.3. MRI acquisition and processing

MRI examinations were performed on a 1.5 T Gyroscan Intera system (Philips Medical Systems) with a quadrature head coil. The morphological protocol consisted of 3-dimensional high-resolution T1-weighted images acquired using magnetization prepared rapid gradient echo (TR = 8.5 ms, TE = 3.9 ms, $\alpha = 10^{\circ}$, FOV = 240 mm, voxel size = $0.94 \times 0.94 \times 1$ mm^3). The same scanner and the same sequence were used for the baseline and the 4-year follow-up MRI.

For cortical and hippocampal volumetric analyses, T1-weighted images were processed using the volBrain system (http://volbrain.upv.es) (Manjón and Coupé, 2016). Recently, volBrain pipeline was compared with well-known tools used on MR brain analysis (SPM, FSL, and FreeSurfer), showing significant improvements in terms of both accuracy and reproducibility for intrascanner and interscanner scan-rescan acquisition (Manjón et al., 2010a) (Næss-Schmidt et al., 2016), even if it was not specifically designed to reduce intraindividual variability and noise with longitudinal registration approach. After denoising (Manjón et al., 2010b), images were corrected for inhomogeneity (Tustison et al., 2010), intensity-normalized (Nyúl and Udupa, 1999), and affine-registered into the Montreal Neurological Institute space (Avants et al., 2011). Then, intracranial cavity was segmented using NICE method (Manjón et al., 2014), and tissue classification (including cortical segmentation) was performed using TMS method (Manjón et al., 2010b). The cortical gray matter volume was calculated as the global gray matter volume minus the deep gray matter volumes (i.e., caudate, thalamus, accumbens, globus pallidus, putamen, hippocampus, and amygdala) (Coupé et al., 2017). Hippocampus was automatically segmented with a patch-based multitemplate method that uses expert manual segmentations in Montreal Neurological Institute space as priors (Coupé et al., 2011). Anatomical boundaries of the hippocampus were defined according to the European Alzheimer's Disease Consortium and Alzheimer's Disease Neuroimaging Initiative Harmonized Protocol (Frisoni et al., 2015). To control for variation in head size, hippocampal and cortical volumes were normalized using the intracranial cavity volume (ICV) of each subject, to express volumes as a proportion of ICV.

The definition of longitudinal evolution of HV/CTV ratio was adapted from previous cross-sectional studies having investigated brain atrophy subtypes in Alzheimer's disease (also known as Murray-Dickson subtypes) because this MRI-based algorithm is able to reliably track the distribution of neurofibrillary tangles in Alzheimer's disease (Risacher et al., 2017; Whitwell et al., 2012). These previous studies defined "limbic predominant," "hippocampal sparing," and "typical" patterns of atrophy according to cross-sectional measures of brain volumes (a 2-step procedure based on splitting participants according to [1] the 25th and 75th percentiles of HV/CTV ratio and [2] the normalized median hippocampal and cortical volumes). Because in the present study we performed our analyses on a population-based sample including healthy people and considered longitudinal changes, we categorized brain atrophy as follows: "hippocampal predominant atrophy," "cortical predominant atrophy," "homogenous atrophy," and "no evidence of specific brain subtype atrophy" based on the longitudinal evolution of this ratio. We calculated HV/CTV ratio on baseline MRI and 4-year follow-up MRI. The difference between these 2 ratios (Δ[HV/CTV ratio]) was considered as a measure of the dynamics of preferential brain atrophy. Participants with Δ(HV/CTV ratios) below the 25th percentile were considered as having "cortical predominant atrophy" if their normalized cortical volume after 4-year follow-up was less than the median value of the whole group and if their normalized hippocampal volume was greater than the median volume of the whole group of participants. Participants with Δ(HV:CTV ratios) above the 75th percentile were considered as having "hippocampal predominant atrophy" if their normalized hippocampal volume after 4-year follow-up was less than the median value of the whole group and if their normalized cortical

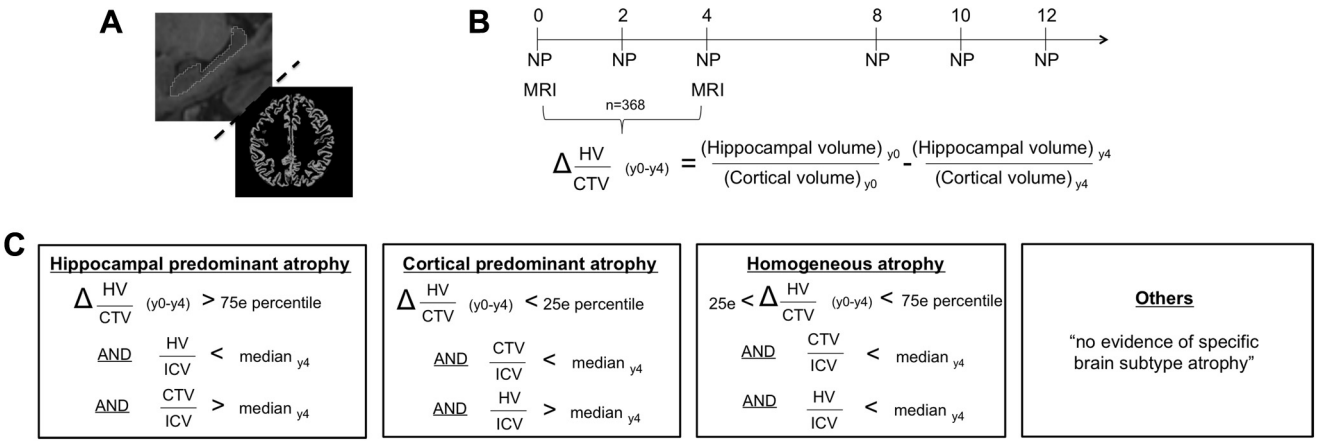

Fig. 1. Methodology of the study. (A) Hippocampal and cortical volumes were measured using the volBrain software and hippocampal-to-cortical volume ratio (HV/CTV) was calculated. (B) During the 12-year follow-up period, neuropsychological assessments were administered at baseline and after 2, 4, 8, 10, and 12 years. We measured HV/CTV on baseline MRI and on 4-year follow-up MRI. The difference between these 2 ratios (Δ(HV/CTV)) was considered as a measure of the dynamics of preferential brain atrophy. (C) The dynamics of brain atrophy was defined according to an algorithm adapted from one recently proposed for tau neuropathology. We defined 4 groups of participants, with either "hippocampal predominant atrophy," "cortical predominant atrophy," "homogenous atrophy," or "no evidence of specific brain subtype atrophy" regarding Δ(HV/CTV) and normalized hippocampal and cortical volumes (see methods). Abbreviations: CTV, cortical volume; HV, hippocampal volume; ICV, intracranial cavity volume; NP, neuropsychological assessment.

volume was greater than the median volume of the whole group of participants. Participants with Δ(HV/CTV ratios) between the 25th and the 75th percentile were considered as having "homogenous atrophy" if their normalized cortical volume after 4-year follow-up was less than the median value of the whole group and if their normalized hippocampal volume was less than the median volume of the whole group of participants. Finally, participants were considered as having "no evidence of specific brain subtype atrophy" if they were not classified in the previous categories (Fig. 1).

2.4. Statistical analyses

Statistical analyses were performed with Prism software 6 (GraphPad) and XLSTATS 19.4 (Addinsoft). The distribution of all continuous data was tested with the Shapiro-Wilk test. We first compared clinical and imaging characteristics at baseline between the 4 groups of participants by using the χ^2 test for categorical variables, and ANOVA or the Kruskal-Wallis test (when assumptions of ANOVA were not met) for continuous variables, followed by appropriate post hoc multiple comparisons tests (Tukey-Kramer or Dunn test, respectively). Second, annual cognitive decline for each test has been calculated for each participant using linear mixed model and compared between groups using analyses of covariance (using age, gender, educational level, and ApoE4 genotype as covariates). Third, the association between brain atrophy subtype and incident Alzheimer's clinical syndrome at follow-up was tested using a log-rank test for trend comparing estimates of the Kaplan-Meier survival analysis. Finally, brain atrophy subtypes (or hippocampal and cortical atrophy rates as continuous variables) and usual risk factors of Alzheimer's disease (age, gender, educational level and APoE4 genotype) were tested to predict time to occurrence of possible or probable Alzheimer's disease using Cox proportional hazard models. All tests were 2-sided, with a type I error set at $\alpha = 0.05$.

3. Results

3.1. Demographical, neuropsychological, and MRI characteristics at baseline

Of the 368 participants included in the analyses, 34 (9.2%) met the criteria defining the "hippocampal predominant atrophy" subtype, 43 (11.7%) met the criteria for "cortical predominant atrophy," and 46 (12.5%) for "homogeneous atrophy." Then, 245 participants (66.6%) were classified as having "no evidence of specific brain subtype atrophy." The characteristics of the sample by atrophy subtypes at baseline are summarized in Table 1. Participants with "hippocampal predominant atrophy" were significantly older than all the other groups ($p = 0.0026$) and had poorer performances on verbal episodic memory tests (both the free and total recall of the FCSRT, $\eta^2 = 0.065$, $p < 0.001$ and $\eta^2 = 0.089$, $p < 0.001$, respectively) and verbal fluency tests (both IST-15 and 60, $\eta^2 = 0.024$, $p = 0.033$ and $\eta^2 = 0.019$, $p = 0.043$, respectively). Participants with "hippocampal predominant atrophy" and "homogeneous atrophy" already had significant lower normalized hippocampal volumes at baseline (especially the homogeneous atrophy group) ($\eta^2 = 0.11$, $p < 0.001$). In contrast, the "cortical predominant atrophy" group did not differ from the other groups at baseline for cortical volumes (Table 1).

3.2. MRI volumes after 4 years

As expected on the MRI performed at 4-year follow-up, the "hippocampal predominant atrophy" and the "homogeneous atrophy" groups had significantly lower normalized hippocampal volumes (both 0.48% of ICV, compared with 0.56% and 0.54% in the 2 other groups, $\eta^2 = 0.24$, $p < 0.001$). The "cortical predominant atrophy" and the "homogeneous atrophy" groups had significantly lower normalized cortical volumes on this follow-up MRI (37.1% and 38.3%, respectively, compared with 42.7% and 40.0% in the "hippocampal predominant atrophy" group and the group with all other participants, $\eta^2 = 0.13$, $p < 0.001$). Individual trajectories of normalized hippocampal and cortical volumes are depicted in Fig. 2.

3.3. Cognitive decline over 12 years

Of the 368 participants included in the analyses, 343 (93.2%) were seen at least one time after the second MRI for a new neuropsychological assessment. Regarding participants lost to follow-up, there was no difference between brain atrophy subtypes, with 2 participants lost to follow-up in the "hippocampal predominant atrophy" group, 3 in the "hippocampal predominant atrophy" group, 4 in the "homogeneous atrophy" group, and 16 in the "no evidence of specific brain subtype atrophy" group (χ^2 test, $p = 0.95$). Among the 25 participants who were not seen after the second MRI, 18 had died.

Table 1
Clinical, neuropsychological, and MRI features of the studied populations at baseline

	Hippocampal predominant atrophy (n = 34)	Cortical predominant atrophy (n = 43)	Homogeneous atrophy (n = 46)	Others (n = 245)	*p* value[b]
Demographical variables at baseline					
Age, mean (SD)	74.3 (3.9)[c,e,h]	71.1 (3.1)	72.0 (3.6)	72.2 (3.9)	0.0026
Gender, women, %	50.0%	48.8%	42.6%[c]	63.4%	0.029
ApoE (ε4 +/− or +/+), %	29.4%	18.6%	11.1%	22.4%	0.21
Education level, high[a], %	44.1%	39.5%	50.0%	48.0%	0.43
Neuropsychological tests at baseline					
MMSE, median [range]	28 [24–30]	29 [25–30]	29 [24–30]	28 [24–30]	0.091
FCSRT, free recall, mean (SD)	20.5 (7.2)[d,g,i]	27.0 (5.1)	24.8 (6.3)	25.1 (5.6)	<0.001
FCSRT, total recall, median [range]	43 [19–48][c,e]	46 [37–48]	46 [33–48]	46 [30–48]	<0.001
BVRT, median [range]	11 [6–15]	12 [8–15]	12 [7–15]	12 [6–15]	0.067
Isaac set test 15 s, mean (SD)	28.9 (5.1)[c]	30.5 (4.4)	30.8 (5.6)	31.8 (6.1)	0.033
Isaac set test 30 s, mean (SD)	43.4 (8.0)	47.5 (6.9)	47.9 (8.4)	47.8 (9.7)	0.074
Isaac set test 60 s, mean (SD)	63.2 (14.5)[c]	70.4 (10.6)	71.0 (13.8)	70.9 (15.4)	0.043
TMT-A, mean (SD)	4.7 (1.4)	5.1 (1.5)	5.0 (1.4)	4.8 (1.5)	0.49
TMT-B, mean (SD)	2.4 (1.1)	2.0 (1.0)	2.4 (1.1)	2.3 (1.2)	0.31
MRI volumes at baseline					
Hippocampal volume, mean % ICV (SD)	0.54 (0.07)[e]	0.58 (0.03)	0.51 (0.05)[d,f]	0.56 (0.01)	<0.001
Cortical volume, mean % ICV (SD)	40.1 (7.2)	42.1 (2.2)	40.1 (2.6)	39.8 (6.3)	0.12

Key: BVRT, benson visual retention test; FCSRT, free and cued selective reminding test; ICV, intracranial cavity volume; MMSE, mini-mental state examination; SD, standard deviation; TMT, trail-making test.
[a] Education level was considered as high or low according to French baccalaureate (equivalent to A-level).
[b] *p*-values refer to χ^2 test for categorical variables and ANOVA or the Kruskal-Wallis test for ordinal variables.
[c] $p < 0.05$ versus "others".
[d] $p < 0.01$ versus "others".
[e] $p < 0.05$ versus "cortical predominant atrophy".
[f] $p < 0.01$ versus "cortical predominant atrophy".
[g] $p < 0.001$ versus "cortical predominant atrophy".
[h] $p < 0.05$ versus "homogeneous atrophy".
[i] $p < 0.01$ versus "homogeneous atrophy" (χ^2 test or post hoc Tukey-Kramer or Dunn tests, as appropriate).

For each neuropsychological test, the slope of cognitive decline over 12 years (assessment at baseline and after 2, 4, 8, 10 and 12 years) was modeled for each participant using mixed effect models and compared between groups after adjustment for age, gender, educational level, and ApoE4 genotype (Fig. 3). We found that participants with "hippocampal predominant atrophy" decline faster than all other groups regarding global cognition (Mini-Mental State Evaluation, $\beta = 0.13$, $p = 0.013$), verbal episodic memory (FCSRT free recall, $\beta = 0.12$, $p = 0.023$ and FCSRT total recall, $\beta = 0.15$, $p = 0.009$), and verbal fluency (IST-30, $\beta = 0.11$, $p = 0.030$ and IST-60, $\beta = 0.13$, $p = 0.011$). Participants with "homogeneous atrophy" decline faster than the other groups on a visuospatial perception and memory test (the Benton Visual Retention Test, $\beta = 0.016$, $p = 0.015$). No atrophy subtype was associated with faster decline on attention or executive functions, regarding TMT-A and TMT-B.

3.4. Incident Alzheimer's disease

After 12 years, we identified 37 cases of Alzheimer's clinical syndrome, 3 cases of Parkinson's disease, 3 cases of possible or probable Lewy-body dementia, and 2 cases of probable frontotemporal lobar degeneration. The proportion of participants who develop Alzheimer's clinical syndrome was 44% in the "hippocampal predominant atrophy" group, 9% in the "cortical predominant atrophy" group, 17% in the "homogeneous atrophy" group, and 7% in the "no evidence of specific brain subtype atrophy" group. Kaplan–Meier survival curves of time to incident Alzheimer's clinical syndrome comparing the 4 groups of brain atrophy subtypes are shown in Fig. 4. Comparing to the 3 other groups, the log-rank test was significant for participants with "hippocampal predominant atrophy" ($\chi^2 = 38.0$, $p < 0.001$).

The results of Cox proportional hazards models investigating the risk of developing Alzheimer's clinical syndrome in our cohort regarding age, gender, educational level, ApoE4 genotype, and brain atrophy subtype are shown in Table 2. "Hippocampal predominant atrophy" was associated with increased risk of developing Alzheimer's clinical syndrome over time (hazard ratio [HR] = 5.73; 95% CI 2.71–12.15), independently of age and ApoE genotype, the 2 other significant predictive factors (HR = 1.19; 95% CI 1.08–1.30 and HR = 2.56; 95% CI 1.27–5.16, respectively).

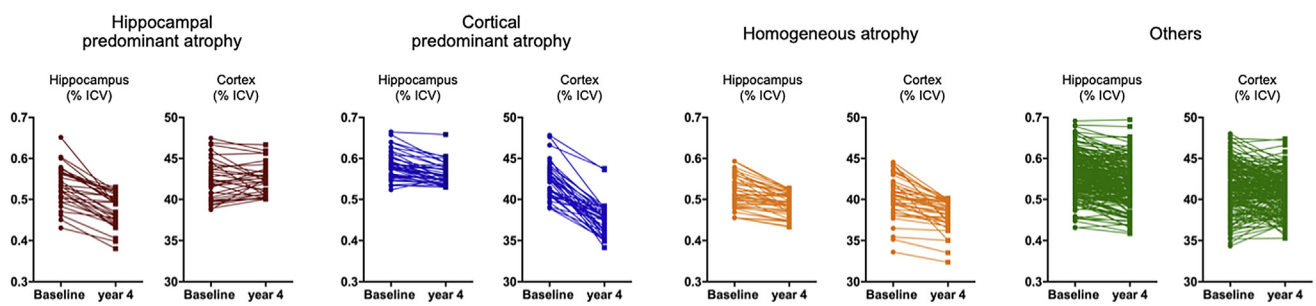

Fig. 2. Spaghetti plots of hippocampal and cortical volumes at baseline and 4 years later. Each line represents one participant. Abbreviation: ICV, intracranial cavity volume.

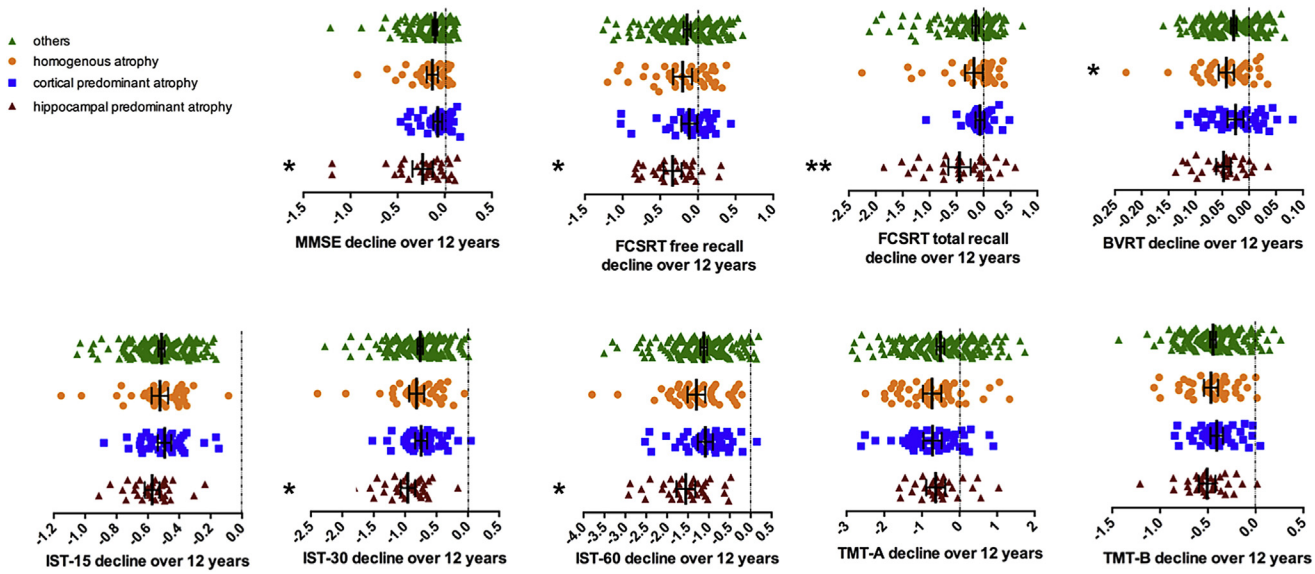

Fig. 3. Dot plots representation of cognitive decline over 12 years in the 4 groups of participants. Dots represent the values of individual slope. Dots represent individual value of longitudinal cognitive decline (mixed effects model) and lines represent the mean decline of the group +/− SEM. Longitudinal cognitive decline between groups was compared using analyses of covariance with age, gender, educational level, and ApoE genotype as covariates: $^{*}p < 0.05$, $^{**}p < 0.01$. Abbreviations: BVRT, Benton Visual Retention Test; FCSRT, Free and Cued Selective Reminding Test; IST, Isaacs Set Test (15, 30, and 60 seconds); MMSE, Mini-Mental State Examination; TMT, Trail-Making Test (parts A and B).

As a sensitivity analysis, we also studied the proportion of participants who develop Alzheimer's clinical syndrome only after the 4-year follow-up visit (i.e., after the second MRI). The log-rank test was still significant for participants with "hippocampal predominant atrophy" compared with the 3 other groups ($\chi^2 = 20.3$, $p < 0.001$). Regarding the Cox proportional hazards models investigating the risk of developing Alzheimer's clinical syndrome over time, "hippocampal predominant atrophy" was associated with increased risk after the 4-year follow-up visit (HR = 6.00; 95% CI 2.67–13.49) independently of the age and ApoE4 genotype.

When hippocampal and cortical atrophy rates were included as continuous variables into the Cox proportional hazards models (instead of brain atrophy subtypes), these MRI measures were not significantly associated with the incidence of Alzheimer's clinical syndrome, alone or in association with confounders.

4. Discussion

In this study, we have adapted the cross-sectional Murray-Dickson algorithm defining "typical," "hippocampal sparing," and "limbic predominant" pathology in patients with Alzheimer's disease (Byun et al., 2015; Murray et al., 2011; Risacher et al., 2017; Whitwell et al., 2012) to longitudinal MRI data gathered from a population-based cohort of nondemented elderly people with a long-term prospective neuropsychological follow-up. We found that participants with "hippocampal predominant atrophy" decline faster than all other groups regarding global cognition, verbal fluency, and verbal episodic memory (even when compared with participants with "homogenous atrophy" who had smaller hippocampal volumes at baseline). Furthermore, we found that the "hippocampal predominant atrophy" group had a much higher risk to develop Alzheimer's clinical syndrome over time, independently of age, gender, educational level, and ApoE4 genotype.

MRI measures of differential hippocampal-to-cortical atrophy have been demonstrated to be a surrogate of neurofibrillary tangles deposits in neuropathologically defined patients with Alzheimer's disease (Whitwell et al., 2012). Thus, we can assume that the differential hippocampal vulnerability measured in the "hippocampal predominant atrophy" group is linked to the early tauopathy defining Braak stages I and II. In this study, which allows a real unbiased prospective assessment of the preclinical phase of Alzheimer's disease, we demonstrated that this differential and specific hippocampal atrophy (related to cortical atrophy) can precede the diagnosis of dementia for up to 8–12 years. In this context, our results are a rare longitudinal and in vivo support of current models of Alzheimer's disease pathophysiology (Jack et al., 2010; Sperling et al., 2011). Indeed, these models postulate that the spreading of neurofibrillary tangles occurs years before dementia, with a stereotypical pattern of early medial temporal lobe involvement (entorhinal cortex and hippocampus), followed by progressive neocortical damage, according to Braak staging (Braak and Braak, 1991). However, these conclusions were to date mostly based on cross-sectional studies, in which longitudinal changes were inferred by studying individuals at different stages of the disease (i.e., controls, mild cognitive impairment, and Alzheimer's disease groups) (Fotenos et al., 2005; Tabatabaei-Jafari et al., 2015).

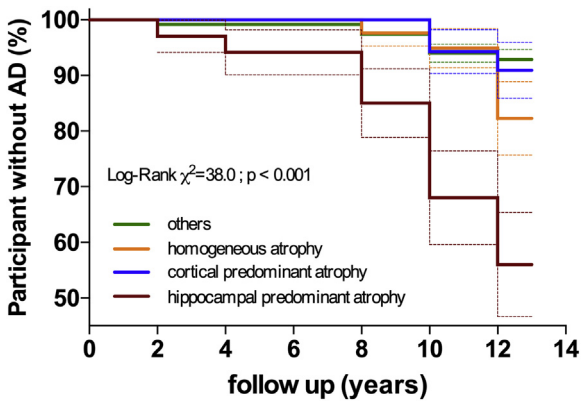

Fig. 4. Kaplan-Meier survival curves representing the incidence of Alzheimer's disease (AD) during the 12-year follow-up period, regarding the dynamics of initial brain subtype atrophy. The dashed lines represent standard errors.

Table 2
Predictive values of age, gender, educational level, ApoE4 genotype alone (model 1) and in combination with brain atrophy subtype (model 2) on time to incident Alzheimer's disease (Cox models, n = 368)

	Hazard ratio	95% CI
Model 1		
Age	1.20	1.10–1.30
Gender	ns	ns
Education level	ns	ns
ApoE4 genotype	2.43	1.22–4.85
Model 2		
Age	1.19	1.08–1.30
Gender	ns	ns
Education level	ns	ns
ApoE4 genotype	2.56	1.27–5.16
Homogeneous atrophy	ns	ns
Cortical predominant atrophy	ns	ns
Hippocampal predominant atrophy	5.73	2.71–12.15

Previous works studying the differential hippocampal-to-cortical distribution of neurofibrillary tangles or the HV/CTV ratio in patients with Alzheimer's disease or Alzheimer's clinical syndrome concluded that a hippocampal sparing disease process was linked to poorer cognitive and functional prognoses, especially if cortical atrophy predominates in parietal lobes (Na et al., 2016; Risacher et al., 2017; Ten Kate et al., 2018). Indeed, "hippocampal sparing" damage define atypical variants of Alzheimer's disease, known to have faster evolutions because of impairment in executive functions, language or visuospatial abilities, which strongly impact autonomy (Scheltens et al., 2016). In contrast, in our cohort of elderly subjects, "hippocampal predominant atrophy" (rather than "cortical predominant" or "homogeneous atrophy") is associated with a poorer prognosis because it announces a typical form of Alzheimer's disease, by far the most common. Finally, we can conclude that the evolution of HV/CTV ratio on MRI can be seen as both an early and a late marker of the disease process (Frisoni et al., 2010), with a 2-stage evolution. First, hippocampal predominant damage is deleterious during aging or the prodromal stage of the disease because it announces future Alzheimer's disease and then, predominant cortical involvement is deleterious in already diagnosed patients because it signs an atypical evolution or a cortical spreading of the pathophysiological process. Another explanation could be that our study "missed" future Alzheimer's disease with "cortical predominant atrophy" because of its inclusion criteria (individuals aged >65 years). Indeed, previous studies showed that "hippocampal sparing" Alzheimer's disease is associated with early-onset dementia (63 ± 10 years [Murray et al., 2011]).

Regarding neuropsychological functioning, "hippocampal predominant atrophy" group declined faster than all other groups on the IST, a test known to be one of the first to decline in the prodromal phase of Alzheimer's disease (Amieva et al., 2008) (even before tests such as the FCSRT that measures episodic memory and define the classical "amnestic syndrome of hippocampal type" in Alzheimer's disease (Auriacombe et al., 2010; Sarazin et al., 2007). Because IST is a multidetermined test, it has been postulated that its early decline in elderly people could be linked to executive functions and information processing speed impairment because of accelerated age-related damage or to semantic memory impairment due to the insidious accumulation of neurofibrillary pathology in the temporal area (Amieva et al., 2008). Our results argue for the second hypothesis.

In our study, it is interesting to note that the "homogeneous atrophy" group had a lower hippocampal volume at baseline than the "hippocampal predominant atrophy" group. However, the "homogeneous atrophy" group is not at higher risk to develop Alzheimer's clinical syndrome than the "cortical predominant atrophy" group or the group of all other participants because hippocampal atrophy may not be related to Alzheimer's disease tauopathy in these cases. Furthermore, the rate of hippocampal atrophy alone was not a significant predictor of the incidence of Alzheimer's clinical syndrome over time in Cox proportional hazards models (instead of brain atrophy subtype). Thus, it highlights that small hippocampal volumes per se are not real predictors of future Alzheimer's clinical syndromes, but that the measure of a dynamic process leading to the differential atrophy of the hippocampus comparing to the neocortex could be a very good marker instead. These findings are in accordance with clinical practice where hippocampal atrophy in the elderly is known to be poorly specific of Alzheimer's disease or prodromal Alzheimer's disease because it also occurs in neurovascular diseases, neuroinflammatory diseases, bipolar disorder, and schizophrenia or other neurodegenerative processes, such as frontotemporal lobar dementia and Lewy body dementia (Harper et al., 2014). We can envision that the measure of the evolution of HV/CTV ratio in therapeutic clinical trials for preclinical Alzheimer's disease could become a better biomarker than hippocampal volumetry alone, by assessing the dynamics of limbic neurofibrillary tangles spreading. Furthermore, such anatomical classifications of brain atrophy subtypes could also help physicians to identify at-risk individuals with subjective memory impairment or mild cognitive impairment (Jung et al., 2016; Kim et al., 2019).

The strengths of this study are the large sample size, the 12-year follow-up period along with a large neuropsychological battery, the few lost to follow-up participants, the longitudinal measure of brain atrophy progression with the same scanner across both time points and the population-based, natural history design. Because the inclusion period of this study was 1999–2000, its first limitation is the lack of assessment of amyloid pathology using positron emission tomography (PET) imaging or cerebrospinal fluid biomarkers, to explore the temporal link between HV/CTV ratio evolution and amyloid-β deposits. In addition, these biomarkers would have specified the diagnosis of Alzheimer's disease, which was in this study only based on clinical criteria. However, the diagnosis of Alzheimer's clinical syndrome (possible or probable Alzheimer's disease according to 1984 and 2011 criteria) was done in our cohort by a panel of independent and expert neurologists and are congruent with observations from the literature regarding for instance the larger ratio of subjects with incident Alzheimer's disease presenting at least one ApoE ε4 allele. We also acknowledge that we have not clearly assessed what are the distinct characteristics of the "homogeneous atrophy" and "cortical predominant atrophy" groups, as well as the cause of their distinct pattern of brain atrophy. Indeed, it could be explained by other ongoing neurodegenerative processes or by neurovascular or psychiatric diseases, known to drive slower cognitive decline than Alzheimer's disease. Future studies will need to address these points.

Our approach based on an indirect measure of the neurofibrillary tangles spreading in aging will be probably overcome by the use of PET-tau imaging in the coming decade, if studies with a similar inclusion criteria and follow-up are set up. Regarding recent PET-tau studies, it is indeed interesting to note the strong correlation between localized ^{18}F-AV-1451 uptake and the longitudinal measures of medial temporal lobe atrophy while the correlation was rather weak regarding ^{18}F-AV-1451 uptake and transversal volumetric analyses (Das et al., 2018). These data support the notion that in vivo measures of tau pathology are tightly linked to the local rate of neurodegenerative change measured with longitudinal MRI measures and strongly support our findings. Furthermore, future longitudinal PET-tau studies will be able to address fundamental questions regarding early Alzheimer's disease pathophysiology (Jack et al., 2018b). For instance, recent transversal multimodal studies on patients with Alzheimer's disease or elderly people had

reported exciting findings linking distant Aβ and neurofibrillary tangles interactions with brain hypometabolism and atrophy (Sepulcre et al., 2016; Whitwell et al., 2018).

5. Conclusion

The monitoring of "hippocampal predominant atrophy" using HV/CTV ratio on MRI appears to be a strong predictor of cognitive decline and incident Alzheimer's clinical syndrome, independently of age, gender, educational level, and ApoE4 genotype. This rather simple morphometric analysis probably captures early lesions of tauopathy defining Braak stage I and II, a decade before Alzheimer's disease onset in nondemented people. Longitudinal HV/CTV ratio evolution could become a strong marker to disentangle brain changes in normal aging from the earliest signs of Alzheimer's disease.

Disclosure

The authors declare no competing financial interests relative to the present study.

Acknowledgements

The 3C Study is conducted under a partnership agreement among the *Institut National de la Santé et de la Recherche Médicale* (INSERM), Bordeaux University, and Sanofi. The *Fondation pour la Recherche Médicale* funded the preparation and initiation of the study. The 3C study is also supported by *Caisse Nationale Maladie des Travailleurs Salariés*, *Direction Générale de la Santé*, *Mutuelle Générale de l'Education Nationale*, *Institut de la Longévité, Conseils Régionaux d'Aquitaine et Bourgogne, Fondation de France,* and the Ministry of Research-INSERM Programme "*Cohortes et collections de données biologiques.*" The 10-year and 12-year follow-up have been funded by ANR 2007LVIE 003 and "*Fondation Plan Alzheimer.*" This study was also achieved within the context of Human Brain Project, the Laboratory of Excellence TRAIL ANR-10-LABX-57 for the Big-DataBrain project and the Investments for the future Program IdEx Bordeaux (ANR-10-IDEX-03-02, HL-MRI Project), Cluster of excellence CPU, and the CNRS. VP also received grants from Fondation Bettencourt Schueller (CCA-Inserm-Bettencourt). The sponsors did not participate in any aspect of the design or performance of the study, including data collection, management, analysis, and the interpretation or preparation, review, and approval of the article.

Authors' contributions: VP, FT, J-FD, and GC contributed to conception and design of the study. VP, PC, CH, MLG, HA, J-FD, and GC contributed to acquisition and analysis of data. VP and GC contributed to drafting the article. All authors revised the article for important intellectual contents.

References

3C Study Group, 2003. Vascular factors and risk of dementia: design of the Three-City Study and baseline characteristics of the study population. Neuroepidemiology 22, 316–325.

Amieva, H., Le Goff, M., Millet, X., Orgogozo, J.M., Pérès, K., Barberger-Gateau, P., Jacqmin-Gadda, H., Dartigues, J.F., 2008. Prodromal Alzheimer's disease: successive emergence of the clinical symptoms. Ann. Neurol. 64, 492–498.

Auriacombe, S., Helmer, C., Amieva, H., Berr, C., Dubois, B., Dartigues, J.-F., 2010. Validity of the free and cued selective reminding test in predicting dementia: the 3C study. Neurology 74, 1760–1767.

Avants, B.B., Tustison, N.J., Song, G., Cook, P.A., Klein, A., Gee, J.C., 2011. A reproducible evaluation of ANTs similarity metric performance in brain image registration. Neuroimage 54, 2033–2044.

Braak, H., Braak, E., 1991. Neuropathological stageing of Alzheimer-related changes. Acta Neuropathol. 82, 239–259.

Byun, M.S., Kim, S.E., Park, J., Yi, D., Choe, Y.M., Sohn, B.K., Choi, H.J., Baek, H., Han, J.Y., Woo, J.I., Lee, D.Y., Alzheimer's Disease Neuroimaging Initiative, 2015. Heterogeneity of regional brain atrophy patterns associated with distinct progression rates in Alzheimer's disease. PLoS One 10, e0142756.

Coupé, P., Manjón, J.V., Fonov, V., Pruessner, J., Robles, M., Collins, D.L., 2011. Patch-based segmentation using expert priors: application to hippocampus and ventricle segmentation. Neuroimage 54, 940–954.

Coupé, P., Catheline, G., Lanuza, E., Manjón, J.V., Alzheimer's Disease Neuroimaging Initiative, 2017. Towards a unified analysis of brain maturation and aging across the entire lifespan: a MRI analysis. Hum. Brain Mapp. 38, 5501–5518.

Das, S.R., Xie, L., Wisse, L.E.M., Ittyerah, R., Tustison, N.J., Dickerson, B.C., Yushkevich, P.A., Wolk, D.A., Alzheimer's Disease Neuroimaging Initiative, 2018. Longitudinal and cross-sectional structural magnetic resonance imaging correlates of AV-1451 uptake. Neurobiol. Aging 66, 49–58.

Dickerson, B.C., Bakkour, A., Salat, D.H., Feczko, E., Pacheco, J., Greve, D.N., Grodstein, F., Wright, C.I., Blacker, D., Rosas, H.D., Sperling, R.A., Atri, A., Growdon, J.H., Hyman, B.T., Morris, J.C., Fischl, B., Buckner, R.L., 2009. The cortical signature of Alzheimer's disease: regionally specific cortical thinning relates to symptom severity in very mild to mild AD dementia and is detectable in asymptomatic amyloid-positive individuals. Cereb. Cortex 19, 497–510.

Dickerson, B.C., Brickhouse, M., McGinnis, S., Wolk, D.A., 2017. Alzheimer's disease: the influence of age on clinical heterogeneity through the human brain connectome. Alzheimers Dement. (Amst) 6, 122–135.

Dubois, B., Feldman, H.H., Jacova, C., Hampel, H., Molinuevo, J.L., Blennow, K., DeKosky, S.T., Gauthier, S., Selkoe, D., Bateman, R., Cappa, S., Crutch, S., Engelborghs, S., Frisoni, G.B., Fox, N.C., Galasko, D., Habert, M.-O., Jicha, G.A., Nordberg, A., Pasquier, F., Rabinovici, G., Robert, P., Rowe, C., Salloway, S., Sarazin, M., Epelbaum, S., de Souza, L.C., Vellas, B., Visser, P.J., Schneider, L., Stern, Y., Scheltens, P., Cummings, J.L., 2014. Advancing research diagnostic criteria for Alzheimer's disease: the IWG-2 criteria. Lancet Neurol. 13, 614–629.

Fotenos, A.F., Snyder, A.Z., Girton, L.E., Morris, J.C., Buckner, R.L., 2005. Normative estimates of cross-sectional and longitudinal brain volume decline in aging and AD. Neurology 64, 1032–1039.

Frisoni, G.B., Fox, N.C., Jack, C.R., Scheltens, P., Thompson, P.M., 2010. The clinical use of structural MRI in Alzheimer disease. Nat. Rev. Neurol. 6, 67–77.

Frisoni, G.B., Jack, C.R., Bocchetta, M., Bauer, C., Frederiksen, K.S., Liu, Y., Preboske, G., Swihart, T., Blair, M., Cavedo, E., Grothe, M.J., Lanfredi, M., Martinez, O., Nishikawa, M., Portegies, M., Stoub, T., Ward, C., Apostolova, L.G., Ganzola, R., Wolf, D., Barkhof, F., Bartzokis, G., DeCarli, C., Csernansky, J.G., deToledo-Morrell, L., Geerlings, M.I., Kaye, J., Killiany, R.J., Lehéricy, S., Matsuda, H., O'Brien, J., Silbert, L.C., Scheltens, P., Soininen, H., Teipel, S., Waldemar, G., Fellgiebel, A., Barnes, J., Firbank, M., Gerritsen, L., Henneman, W., Malykhin, N., Pruessner, J.C., Wang, L., Watson, C., Wolf, H., deLeon, M., Pantel, J., Ferrari, C., Bosco, P., Pasqualetti, P., Duchesne, S., Duvernoy, H., Boccardi, M., EADC-ADNI Working Group on The Harmonized Protocol for Manual Hippocampal Volumetry and for the Alzheimer's Disease Neuroimaging Initiative, 2015. The EADC-ADNI Harmonized Protocol for manual hippocampal segmentation on magnetic resonance: evidence of validity. Alzheimers Dement. 11, 111–125.

Gosche, K.M., Mortimer, J.A., Smith, C.D., Markesbery, W.R., Snowdon, D.A., 2002. Hippocampal volume as an index of Alzheimer neuropathology: findings from the Nun Study. Neurology 58, 1476–1482.

Harper, L., Barkhof, F., Scheltens, P., Schott, J.M., Fox, N.C., 2014. An algorithmic approach to structural imaging in dementia. J. Neurol. Neurosurg. Psychiatry 85, 692–698.

Jack, C.R., Dickson, D.W., Parisi, J.E., Xu, Y.C., Cha, R.H., O'Brien, P.C., Edland, S.D., Smith, G.E., Boeve, B.F., Tangalos, E.G., Kokmen, E., Petersen, R.C., 2002. Antemortem MRI findings correlate with hippocampal neuropathology in typical aging and dementia. Neurology 58, 750–757.

Jack, C.R., Knopman, D.S., Jagust, W.J., Shaw, L.M., Aisen, P.S., Weiner, M.W., Petersen, R.C., Trojanowski, J.Q., 2010. Hypothetical model of dynamic biomarkers of the Alzheimer's pathological cascade. Lancet Neurol. 9, 119–128.

Jack, C.R., Bennett, D.A., Blennow, K., Carrillo, M.C., Dunn, B., Haeberlein, S.B., Holtzman, D.M., Jagust, W., Jessen, F., Karlawish, J., Liu, E., Molinuevo, J.L., Montine, T., Phelps, C., Rankin, K.P., Rowe, C.C., Scheltens, P., Siemers, E., Snyder, H.M., Sperling, R., Contributors, 2018a. NIA-AA Research Framework: toward a biological definition of Alzheimer's disease. Alzheimers Dement. 14, 535–562.

Jack, C.R., Wiste, H.J., Schwarz, C.G., Lowe, V.J., Senjem, M.L., Vemuri, P., Weigand, S.D., Therneau, T.M., Knopman, D.S., Gunter, J.L., Jones, D.T., Graff-Radford, J., Kantarci, K., Roberts, R.O., Mielke, M.M., Machulda, M.M., Petersen, R.C., 2018b. Longitudinal tau PET in ageing and Alzheimer's disease. Brain J 141, 1517–1528.

Jung, N.-Y., Seo, S.W., Yoo, H., Yang, J.-J., Park, S., Kim, Y.J., Lee, J., Lee, J.S., Jang, Y.K., Lee, J.M., Kim, S.T., Kim, S., Kim, E.-J., Na, D.L., Kim, H.J., 2016. Classifying anatomical subtypes of subjective memory impairment. Neurobiol. Aging 48, 53–60.

Kim, H.J., Park, J.-Y., Seo, S.W., Jung, Y.H., Kim, Y., Jang, H., Kim, S.T., Seong, J.-K., Na, D.L., 2019. Cortical atrophy pattern-based subtyping predicts prognosis of amnestic MCI: an individual-level analysis. Neurobiol. Aging 74, 38–45.

Manjón, J.V., Coupé, P., 2016. volBrain: an online MRI brain volumetry system. Front Neuroinform. 10, 30.

Manjón, J.V., Coupé, P., Martí-Bonmatí, L., Collins, D.L., Robles, M., 2010a. Adaptive non-local means denoising of MR images with spatially varying noise levels. J. Magn. Reson. Imaging 31, 192–203.

Manjón, J.V., Tohka, J., Robles, M., 2010b. Improved estimates of partial volume coefficients from noisy brain MRI using spatial context. Neuroimage 53, 480–490.

Manjón, J.V., Eskildsen, S.F., Coupé, P., Romero, J.E., Collins, D.L., Robles, M., 2014. Nonlocal intracranial cavity extraction. Int. J. Biomed. Imaging 2014, 820205.
McKhann, G., Drachman, D., Folstein, M., Katzman, R., Price, D., Stadlan, E.M., 1984. Clinical diagnosis of Alzheimer's disease: report of the NINCDS-ADRDA work group under the auspices of department of health and human services task force on Alzheimer's disease. Neurology 34, 939–944.
Murray, M.E., Graff-Radford, N.R., Ross, O.A., Petersen, R.C., Duara, R., Dickson, D.W., 2011. Neuropathologically defined subtypes of Alzheimer's disease with distinct clinical characteristics: a retrospective study. Lancet Neurol. 10, 785–796.
Na, H.K., Kang, D.R., Kim, S., Seo, S.W., Heilman, K.M., Noh, Y., Na, D.L., 2016. Malignant progression in parietal-dominant atrophy subtype of Alzheimer's disease occurs independent of onset age. Neurobiol. Aging 47, 149–156.
Nyúl, L.G., Udupa, J.K., 1999. On standardizing the MR image intensity scale. Magn. Reson. Med. 42, 1072–1081.
Næss-Schmidt, E., Tietze, A., Blicher, J.U., Petersen, M., Mikkelsen, I.K., Coupé, P., Manjón, J.V., Eskildsen, S.F., 2016. Automatic thalamus and hippocampus segmentation from MP2RAGE: comparison of publicly available methods and implications for DTI quantification. Int. J. Comput. Assist. Radiol. Surg. 11, 1979–1991.
Risacher, S.L., Anderson, W.H., Charil, A., Castelluccio, P.F., Shcherbinin, S., Saykin, A.J., Schwarz, A.J., Alzheimer's Disease Neuroimaging Initiative, 2017. Alzheimer disease brain atrophy subtypes are associated with cognition and rate of decline. Neurology 89, 2176–2186.
Sarazin, M., Berr, C., De Rotrou, J., Fabrigoule, C., Pasquier, F., Legrain, S., Michel, B., Puel, M., Volteau, M., Touchon, J., Verny, M., Dubois, B., 2007. Amnestic syndrome of the medial temporal type identifies prodromal AD: a longitudinal study. Neurology 69, 1859–1867.
Scheltens, P., Blennow, K., Breteler, M.M.B., de Strooper, B., Frisoni, G.B., Salloway, S., Van der Flier, W.M., 2016. Alzheimer's disease. Lancet 388, 505–517.
Sepulcre, J., Schultz, A.P., Sabuncu, M., Gomez-Isla, T., Chhatwal, J., Becker, A., Sperling, R., Johnson, K.A., 2016. In vivo tau, amyloid, and gray matter profiles in the aging brain. J. Neurosci. 36, 7364–7374.
Sperling, R.A., Aisen, P.S., Beckett, L.A., Bennett, D.A., Craft, S., Fagan, A.M., Iwatsubo, T., Jack, C.R., Kaye, J., Montine, T.J., Park, D.C., Reiman, E.M., Rowe, C.C., Siemers, E., Stern, Y., Yaffe, K., Carrillo, M.C., Thies, B., Morrison-Bogorad, M., Wagster, M.V., Phelps, C.H., 2011. Toward defining the preclinical stages of Alzheimer's disease: recommendations from the National Institute on Aging-Alzheimer's Association workgroups on diagnostic guidelines for Alzheimer's disease. Alzheimers Dement. 7, 280–292.
Tabatabaei-Jafari, H., Shaw, M.E., Cherbuin, N., 2015. Cerebral atrophy in mild cognitive impairment: a systematic review with meta-analysis. Alzheimers Dement. (Amst) 1, 487–504.
Ten Kate, M., Dicks, E., Visser, P.J., van der Flier, W.M., Teunissen, C.E., Barkhof, F., Scheltens, P., Tijms, B.M., Alzheimer's Disease Neuroimaging Initiative, 2018. Atrophy subtypes in prodromal Alzheimer's disease are associated with cognitive decline. Brain 141, 3443–3456.
Tustison, N.J., Avants, B.B., Cook, P.A., Zheng, Y., Egan, A., Yushkevich, P.A., Gee, J.C., 2010. N4ITK: improved N3 bias correction. IEEE Trans. Med. Imaging 29, 1310–1320.
Whitwell, J.L., Dickson, D.W., Murray, M.E., Weigand, S.D., Tosakulwong, N., Senjem, M.L., Knopman, D.S., Boeve, B.F., Parisi, J.E., Petersen, R.C., Jack, C.R., Josephs, K.A., 2012. Neuroimaging correlates of pathologically defined subtypes of Alzheimer's disease: a case-control study. Lancet Neurol. 11, 868–877.
Whitwell, J.L., Graff-Radford, J., Tosakulwong, N., Weigand, S.D., Machulda, M., Senjem, M.L., Spychalla, A.J., Vemuri, P., Jones, D.T., Drubach, D.A., Knopman, D.S., Boeve, B.F., Ertekin-Taner, N., Petersen, R.C., Lowe, V.J., Jack, C.R., Josephs, K.A., 2018. Imaging correlations of tau, amyloid, metabolism, and atrophy in typical and atypical Alzheimer's disease. Alzheimers Dement. 14, 1005–1014.